Journal of Korean Society of Remote Sensing, Vol. 4, No. 1, 1988

Microwave Radar Backscatter Model of Multiyear Sea Ice

Young Soo Kim
Department of Electrical Engineering
Pohang Institute of Science & Technology
Pohang, Korea
(Received September 1, 1987; Accepted January 15, 1988)

Abstract

Multiyear ice is quite thick in general, and it needs to be distinguished from thinner types of ice because it represents a severe navigational hazard. Here, models are described for the radar backscatter from multiyear sea ice, based on simple scattering layers. Under cold conditions, the radiative transfer volume-scatter model can describe the backscattering from multiyear ice for frequencies higher than about X-band, while the surface scattering contribution has to be included for lower frequencies. A simple semi-empirical model is shown to be a good approximation to the radiative transfer model in describing the volume scattering from multiyear ice.

1. Introduction

Several microwave methods exist for obtaining information from aircraft and spacecraft about the ice cover and adjacent open sea. Passive microwave systems use the difference in emissivity for open water and for different ice types, and they have been shown to be quite useful(Troy et al., 1978). Their inherently poor resolution limits their use, however. Among several active microwave (radar) systems, the synthetic-aperture radar(SAR) has the greatest potential because it provides a map with very fine resolution. Problems still exist, however, in the interpretation of the signatures for different sea ice types and at different frequencies.

In this paper and the companion paper, theoretical models are described to explain the microwave backscattering from sea ice. The two major types of ice, multiyear ice and the first-year ice are characterized with two different backscattering machanisms; surface scattering alone for first-year ice, and combined volume- and surface-scattering for multiyear ice. For first-year ice, it was shown by Kim(1984) that the surface scattering model(physical-optics) alone provides a good fit to measured angular- and frequency- behaviors of the backscattering coefficient σ°.

For multiyear ice, the air bubbles in the recrystallized ice layer in the top portion are assumed

to be the main volume scatterers. The radiative-transfer volume scattering model is shown here to be able to describe the backscattering from multiyear ice for frequencies higher than about X-band. When the frequency is lower and the ice surface is rough, it is shown that the volume-scattering contribution can be smaller than the surface-scattering contribution, and the summation of the two provides a good general agreement with the measured frequency-and angular-behaviors of σ° for multiyear ice.

This paper also presents a simple semi-empirical model to describe the volume-scattering contribution of multiyear ice. The complicated theoretical solution of the radiative transfer equation can be reduced to a simple analytical solution if the multiple scattering and the volume-surface interaction can be neglected(Karam and Fung, 1982). Within the reported ranges of multiyear ice characteristics, the solution using the semi-empirical formulation is shown to be a good approximation to that of formal radiative-transfer model. Using the semi-empirical model, the effect of the size distribution of the air bubbles and the density variation with depth are studied.

2. Volume-Scattering from Multiyear Ice

The large air bubbles found in the multiyear ice are likely to be the major source of volume scattering. However, the snow cover on ice also contributes volume scattering by itself, and modify the backscattering from the ice. These factors were considered in Kim et al.(1984), and it was shown that the effect of dry snow cover on total backscattering from multiyear ice is not severe. For wet snow cover, the σ° approaches the value of thick wet snow layer rapidly as the snow depth is increased.

In this paper, only the snow-free multiyear ice is considered, and a simple two-layer model is proposed. The first layer is the layer of recrystallized ice which contains large air bubbles. The density of this layer is usually reported to be within 0.7 $-$0.8 gm/cm^3, although this is highly variable(Campbell et al., 1978). The salinity of this layer is almost zero, but a slightly higher value(0.7°/oo) has been noted. The depth of this layer can be assumed to be about 20-30 cm, but this milky layer can be as thick as 55 cm(Onstott, 1980). The second layer is the clear ice layer with occasional small air bubbles. This layer can be assumed to be a half-space because microwaves are not expected to reach the ice bottom. This layer has salinity of 1 to 2°/oo, with density of 0.8 to 0.9 gm/cm^3. The first approximation will be to neglect the air bubbles in the second layer, considering only the first layer as the volume scattering layer.

In the radiative-transfer approach, the volume scattering layer is characterized with the scattering albedo ω and the optical depth τ given by

$$\omega = k_s/(k_s + k_a) \quad \ldots\ldots (1)$$

$$\tau = (k_s + k_a)\, d = k_e\, d \quad \ldots\ldots (2)$$

where k_s is the volume scattering coefficient and k_a is the volume absorption coefficient. Here, the extinction coefficient, k_e is assumed to be constant in the layer of depth d. The scattering albedo is determined and affected by; (1)wavelength(frequency), (2)air bubble size, (3)dielectric constant of background ice(which varies with salinity and temperature), and (4)density of the ice from which one can estimate the volume fraction of air bubbles(Vant et al., 1978). These factors are all variables. The optical depth of a layer changes with all the above factors and also with the physical depth of the layer.

Fig. 1 illustrates the effect of dielectric constant, ε_b of the background ice(effect of salinity and temperature) and the density, ρ of the ice on scattering albedo. Here, all the air bubbles were assumed to have the same effective radius. The ε_b' was taken to be 3.15, which is the value for

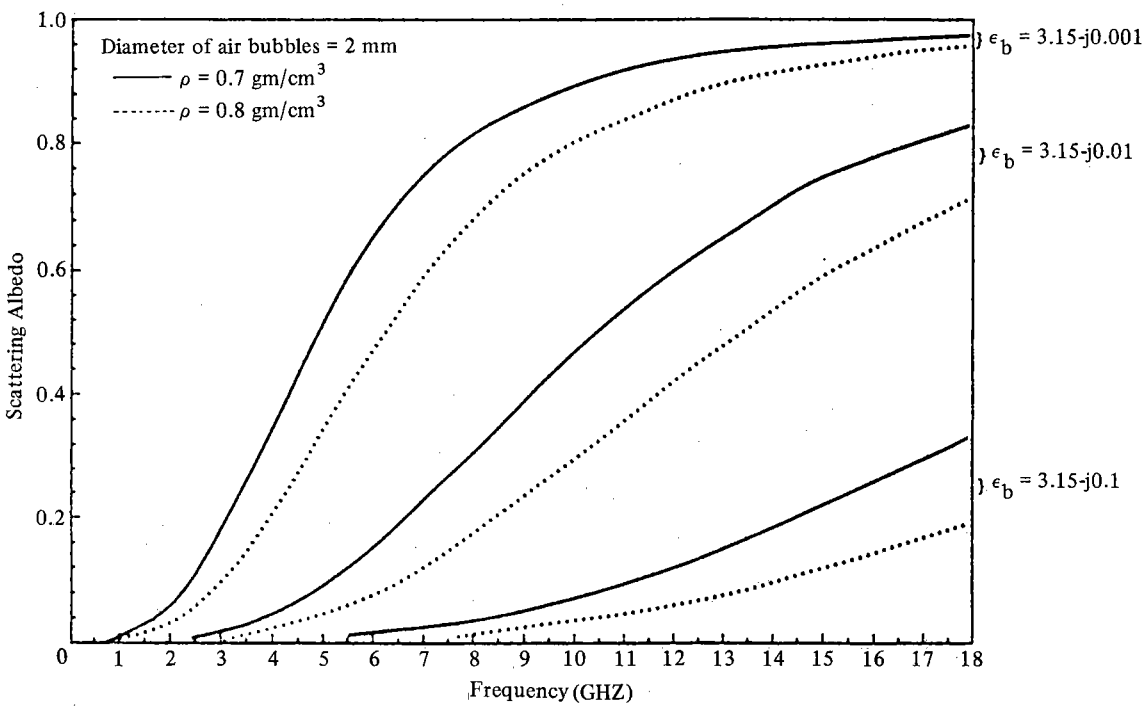

Fig. 1. Scattering Albedo as a Function of Frequency for the Air Bubbles inside the Ice Medium. The effect of change in the dielectric constant of background ice and the effect of different densities are shown.

fresh water ice. The ϵ_b'' was varied from 0.001 to 0.1. The measured values of ϵ_b'' of pure ice (S= 0°/oo) range from about 0.001 to 0.01 in this frequency range, and it may be frequency – and temperature-independent(Ulaby et al., 1986). The behavior, however, is not very well established. When the background ice is saline(up to 0.7°/oo), the ϵ_b'' at 10 GHz can change from 0.01 to 0.1, depending on temperature(Vant et al., 1974, 1978). The value may also be slightly frequency-dependent, but this effect was not included in the calculations. As can be seen from Fig. 1, the salinity and temperature(therefore the ϵ_b'') of the ice can play a major role in determining the scattering albedo. At 10 GHz, it can change from 0.08 to 0.9 when the ϵ_b'' of background ice change from 0.1 to 0.001 as either salinity or temperature changes. The effect of change in the density of ice is not as severe. The size of air bubbles also seems to be a significant factor because at 10 GHz the scattering albedo can change from 0.1 to about 0.76 when the diameter of air bubbles changes from 1 mm to 3 mm when $\epsilon_b = 3.15 - j\ 0.01$ and $\rho = 0.7$ gm/cm^3 (Kim, 1984). A large change in optical depth due to the change in the size of air bubbles was noted for the frequencies higher than about 8 GHz (Kim, 1984).

These changes in the scattering albedo and the optical depth of the volume scattering layer due to the change in the temperature or due to the difference in the salinity, density, etc. result in different volume backscattering coefficient σ° calculated using the radiative-transfer model(Eom, 1982). Figs. 2 and 3 shows the theoretical σ° for the volume scattering layer at 13 GHz with HH-polarization. The volume scattering term interacted with the small-scale roughness of the surface (Eom, 1982) is shown, while the purely surface-scattered term is not included. The surface is characterized with the surface height standard deviation σ and the correlation length ℓ. In Fig. 2,

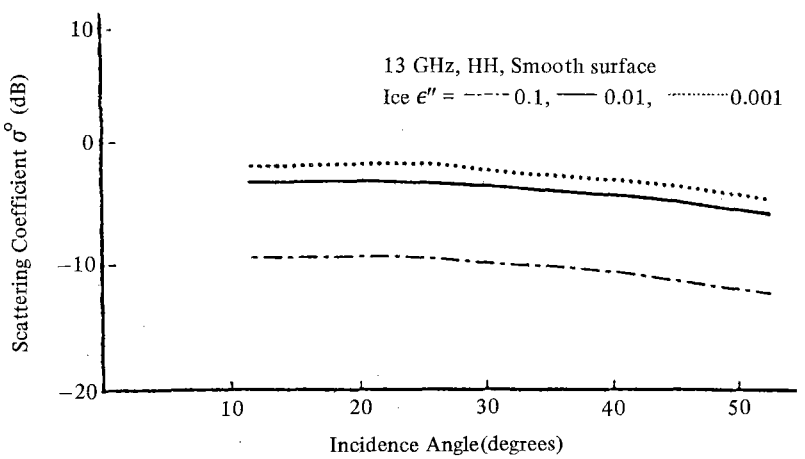

Fig. 2. Theoretical Angular Behavior of σ° for the Volume Scattering Layer. Three curves are for the layers with 3 different ϵ_b''.

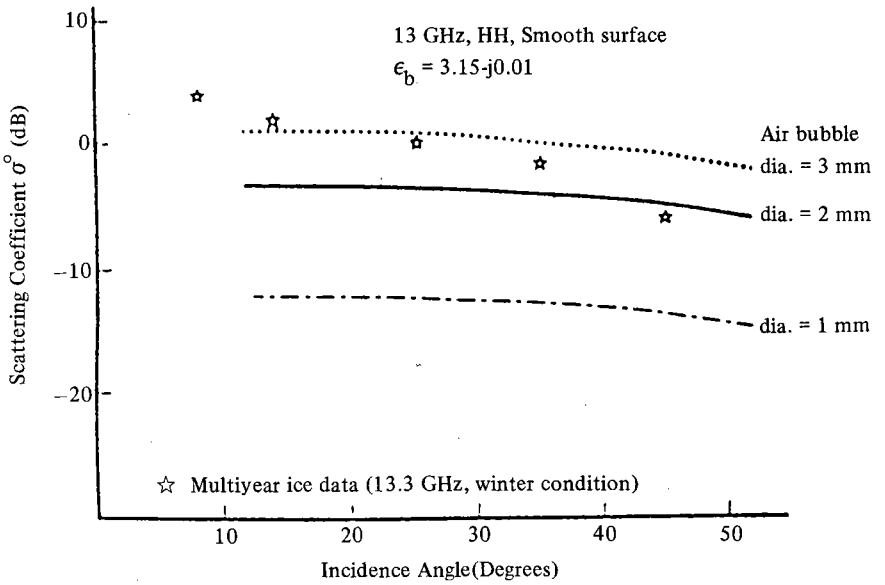

Fig. 3. Theoretical Angular Behaviors of σ° for the Volume Scattering Layer. Three curves with 3 different sizes of the air bubbles are shown. Also shown is the measured multi-year ice data(Gray et al., 1982)

the effect of the ϵ_b'' of the background ice are shown. When the ϵ_b'' reduces from 0.1 to 0.01, the scattering albedo increases from 0.16 to 0.66 at 13 GHz for the layer with 2 mm air bubbles. The resultant σ° increases about 6 dB for all the incidence angles. A rougher surface would reduce the volume scattering contribution to the backscatter direction(Kim, 1984). Fig. 3 shows the effect of air bubble size. The σ° increases as much as 9 dB when the average diameter increases from 1 to 2 mm, and increases further(4 dB) when the diameter increases from 2 to 3 mm. When the depth of the scattering layer is changed from 20 to 50 cm, the σ° increases about 1.5 dB. Increase in density means less volume fraction of the scatterers, and therefore smaller volume-scattering cross section. When the density is increased from 0.7 to 0.8 gm/cm^3, the σ° decreases about 2 to 3 dB. The effect on σ° of the average medium dielectric constant seems to be insignificant in the ranges of values reported(ϵ' = 2.5 to 2.7). Also the effect of ϵ_b' of the nonscattering layer(ϵ_b' = 3.15 to 4.0) seems to be negligible(less than 0.1 dB).

In actual measurements, the purely surface-scattered term not considered so far will also be present and may very well be the dominant factor especially at small incidence angles. The difference in the slopes of the angular behaviors between the measured and the theoretical values of σ° shown in Fig. 3 may have been resulted from the omission of the purely surface-scattered

term in calculation. The change of dominance between the surface- and volume-scattering terms should occur at different incidence angles depending on the surface roughness and the frequency. Fig. 4 shows the theoretical backscattering coefficients of multiyear ice at 8 GHz and 13 GHz. Here surface-scattering terms and volume-scattering terms are shown separately to illustrate the

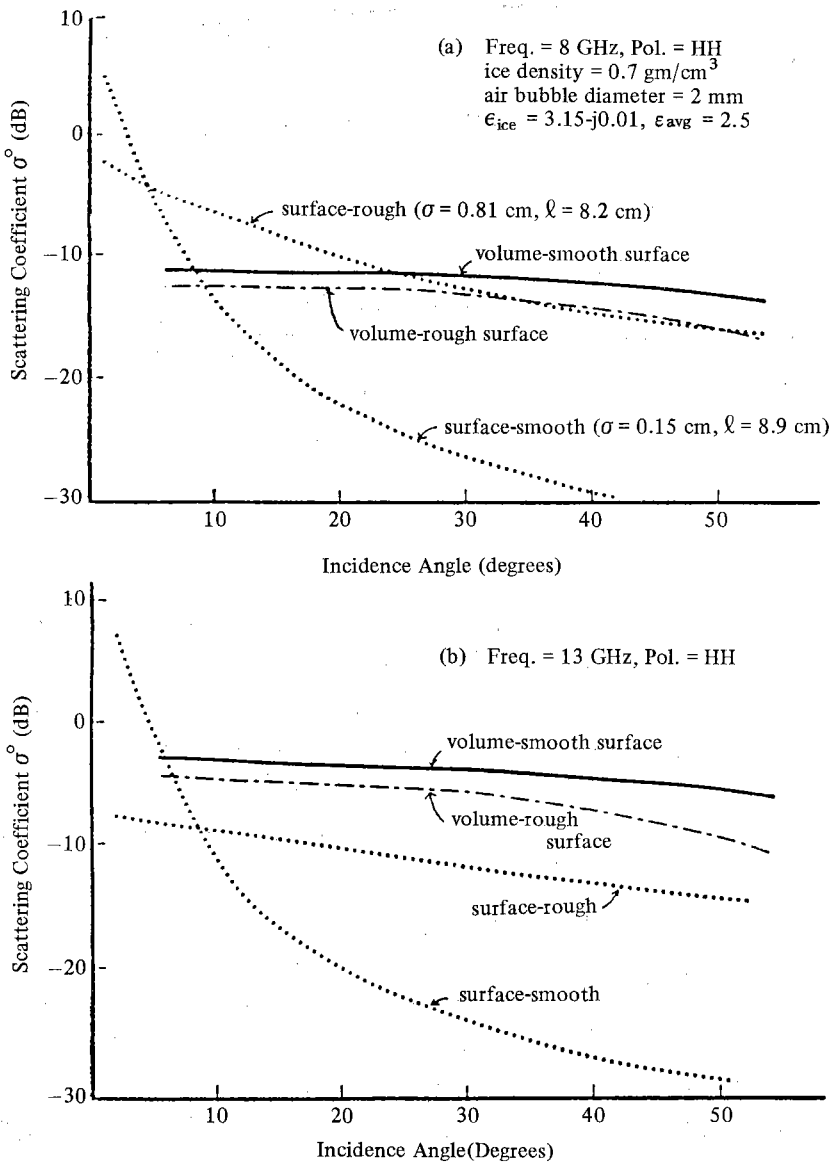

Fig. 4. Theoretical Backscattering Coefficient of Multiyear Ice (a) at 8 GHz, (b) at 13 GHz. Volume- and surface-scattering terms are shown separately to show relative contributions.

relative contributions. The surface-scattering terms are calculated using the physical-optics model with exponential correlation function(Eom, 1982) which was shown by Kim(1984) to be able to predict the signatures from first-year ice. For multiyear ice with a smooth surface, the volume scattering dominates when the incidence angle is larger than about 10° at 8 GHz and about 5° at 13 GHz. For multiyear ice with a rough surface, the surface-scattering term is higher than the volume term until about 30° incidence angle and remains comparable at larger incidence angles at 8 GHz. At 13 GHz, the volume-scattering term is always larger than the surface term except at near nadir.

Fig. 5 shows the theoretical frequency behaviors of the surface– and the volume-scattering terms at the incidence angle of 31 degrees. For multiyear ice with a smooth surface, the volume-scattering term dominates. As the surface becomes rougher, the surface-scattering term increases drastically while the effective volume–scattering term decreases slightly. Therefore, at low microwave frequencies, the surface-scattering term can be larger than the volume term when the incidence angle is 31°. For the physical parameters of multiyear ice shown in the figure, the crossover occurs around 8 GHz.

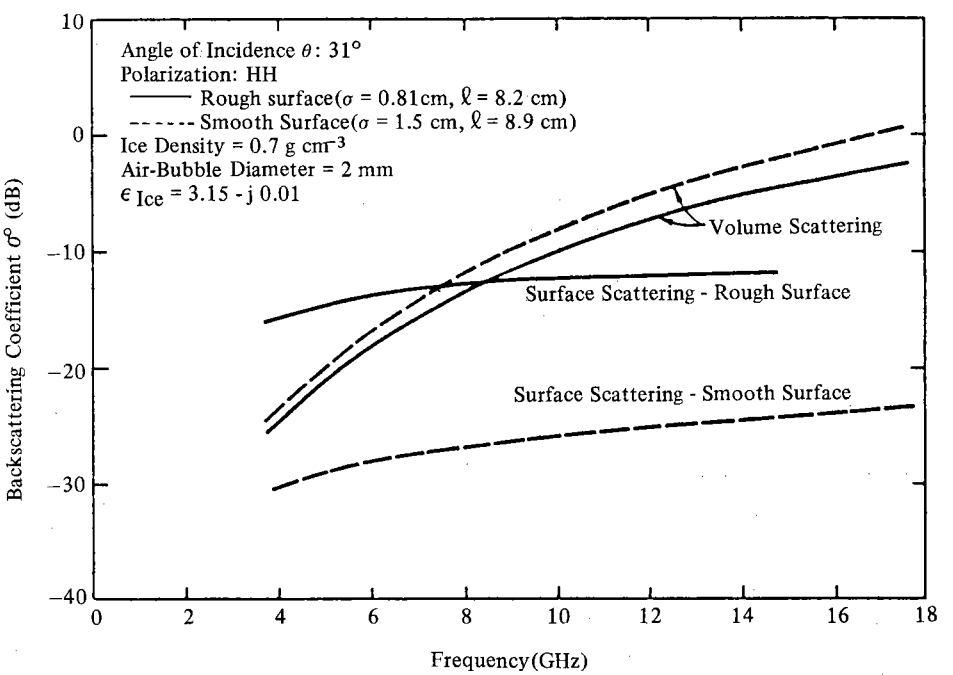

Fig. 5. Theoretical Frequency Response of σ°. The surface- and the volume-scattering terms are plotted separately for two kinds of surface roughness.

Fig. 6 shows the sum of the surface– and volume– scattering terms for multiyear ice with two kinds of surface roughnesses; also shown are several reported measurements of multiyear ice. A good general agreement can be seen, and the radiative-transfer model predicts the angular– and the frequency-behaviors of σ° for multiyear ice satisfactorily.

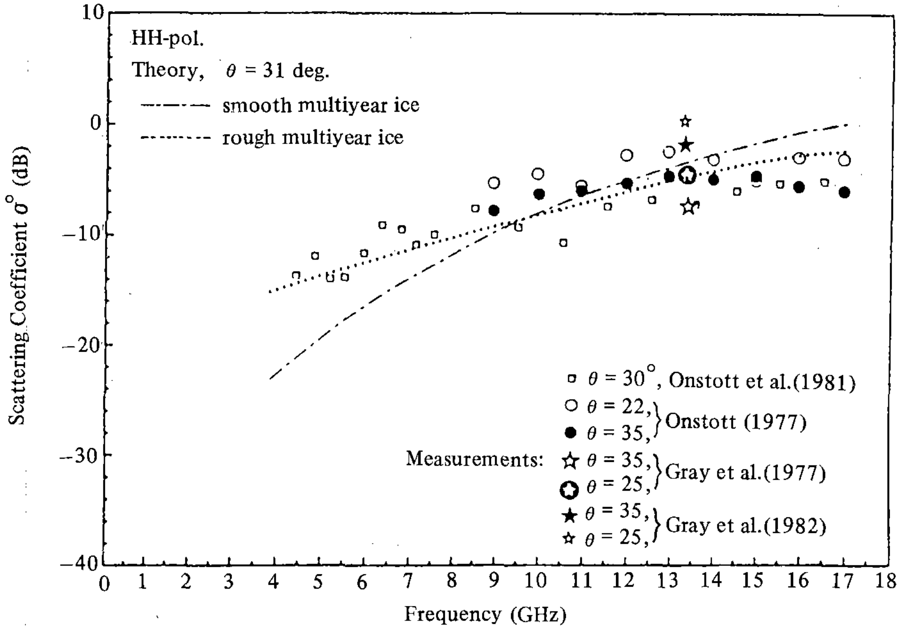

Fig. 6. Calculated and Measured Frequency Responses of σ° of Multiyear Ice with Smooth Surface and Rough Surface.

3. Semi-Empirical Volume Scattering Model of Multiyear Ice

In view of the simple, single-layer model for multiyear ice(no air bubbles in the second layer), the backscattering coefficient has been modeled with the following semi-empirical equation.

$$\sigma^\circ(\theta) = \sigma_S^\circ(\theta) + T^2(\theta)\,\sigma_V^\circ(\theta') \quad \text{.......(3)}$$

where $\sigma_S^\circ(\theta)$ = the backscattering coefficient of the ice surface

$T(\theta)$ = the power transmission coefficient of the upper surface.

$\sigma_V^\circ(\theta')$ = the volume backscattering coefficient of the ice

θ' = the angle of refraction in the ice medium

Karam and Fung(1982) reduced the general theoretical solution of the radiative-transfer equation to the form of Eq.(3) under several simplifying conditions. The factors neglected in this formulation are the terms representing the volume-surface interaction, which maybe significant for cross-polarized scattering. These are the terms scattered by the volume inhomogeneities and reflected by the lower interface. For the multiyear ice problem, the backscattering coefficient of the lower interface(between the recrystallized ice layer and the clear ice layer) would be very small because the interface is arbitrary and the dielectric discontinuity is very small. The volume backscattering coefficient of the ice layer can be found in Ulaby et al. (1982).

$$\sigma_v^\circ(\theta') = \frac{N\,\sigma_b \cos\theta'}{2k_e}\left[1 - \frac{1}{L^2(\theta')}\right] \qquad (4)$$

where N = number of scatterers per unit volume = $f/(4\pi r^3/3)$

f = volume fraction of scatterers (Vant et al., 1978),

= 1 – (ice density) / 0.926

r = radius of scatterer,

σ_b = backscattering cross section of an individual scatterer

= $4\pi r^6 (\epsilon_b')^2 k_o^2 \left|\frac{n^2-1}{n^2+2}\right|^2$

$L(\theta')$ = $\exp(k_e d \sec\theta')$, which represents one-way loss through the layer with extinction coefficient k_e and depth d,

k_o = free space wave number,

n = index of refraction.

In the above equation, all of the scatterers are assumed to be of the same size, and the multiple scattering is neglected. The transmission loss through the upper surface is included in the $T^2(\theta)$-term in Eq.(3), and $T^2(\theta)\ \sigma_v^\circ(\theta')$ is the effective volume scattering term in the σ° seen by the radar. This is calculated, and Fig. 7 shows the comparison of the empirical model behavior with that of the radiative-transfer model. The radiative-transfer model(Eom, 1982) includes the effect of small scale upper surface roughness, while the empirical model does not. As can be seen in the figure, the empirical model prediction matches very well with that of the radiative-transfer model for all the frequencies considered. This similar prediction, especially at low frequencies, might have resulted from the fact that the physical parameters used in the theoretical computation resulted in a small optical depth and scattering albedo at frequencies below about 10 GHz. When this is the case, the scattering process might actually approach single-scattering, and therefore the empirical model can be used to approximate the radiative-transfer model. As the frequency is

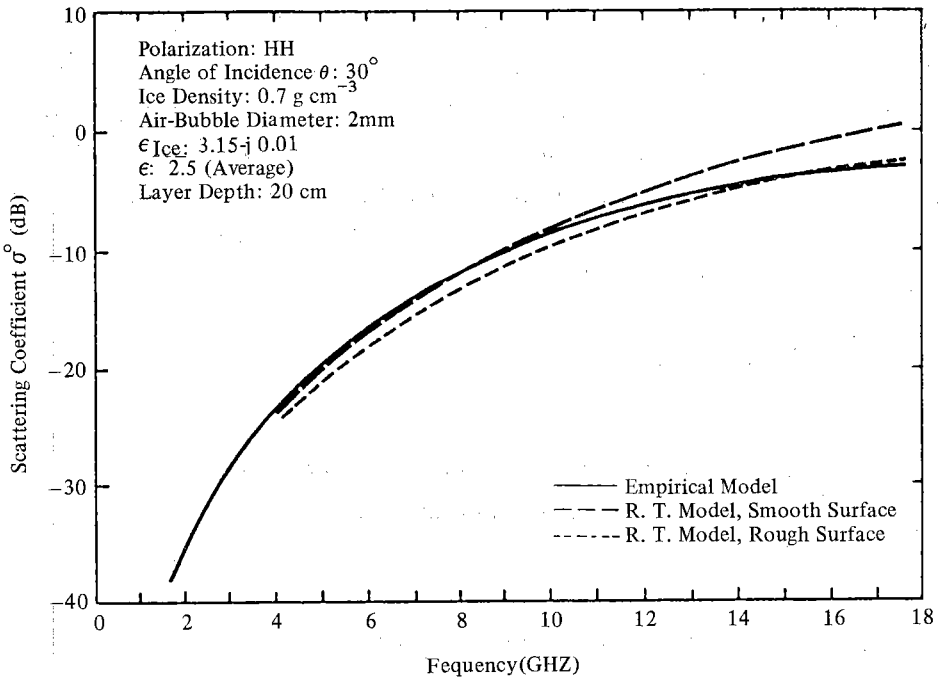

Fig. 7. Comparison of Empirical Model Behavior with that of Radiative-Transfer Model. Empirical model does not include the effect of surface roughness, while the radiative transfer model does.

increased from about 10 GHz, and the scattering albedo and optical depth is increased above certain values, the discrepancy increases as can be seen in Fig. 7(see the theoretical curve for smooth surface and the curve for empirical model). Fig. 8 shows the angular behavior of the empirical model at 13 GHz, HH-polarization. Again, similar results are found for the theoretical model and the empirical model. For all the practical values of physical parameters, the empirical model seems to be able to predict the volume scattering from multiyear ice.

In the above development, a uniform distribution of identical scatterers was assumed for the scattering layer. However, thin sections of ice cores show that the scatterers are actually distributed in size. Moreover, the density varies with depth. These factors are studied further with the empirical model.

The effect of the distribution of the scatterer size could be treated as is done for the scattering due to rain or cloud. For these problems, numerous experiments have been conducted to find the drop size distribution; for air bubbles in the sea ice, only a limited data set is available (Poe et al., 1974, Onstott, 1980). Therefore, only some simple cases in considered. The scattering

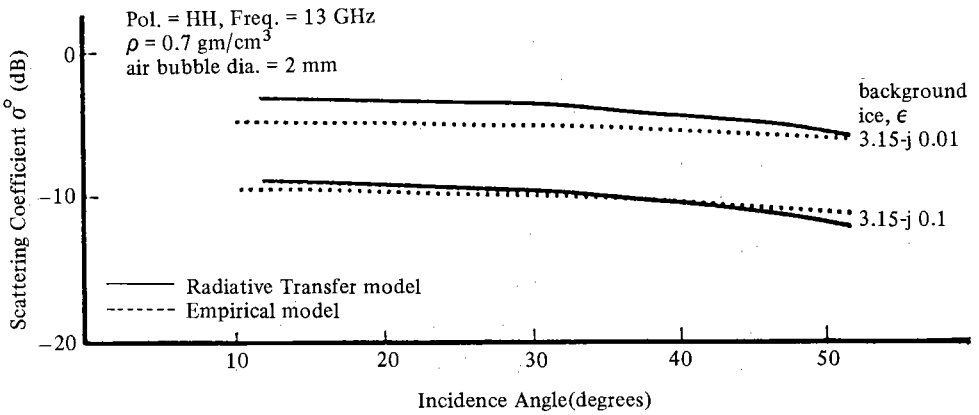

Fig. 8. Comparison of Empirical Model Behavior with that of Radiative-Transfer Model. Shown are the effects of the imaginary part of the dielectric constant of ice. Smooth surface is assumed with the theoretical model(σ = 0.15 cm, ℓ = 8.9 cm).

Table 1. Effect of Scatterer Size Distribution

	Case 1 100% 2mm-diameter air bubbles	Case 2 10% 1mm 80% 2mm 10% 3mm	Case 3 33% 1mm 33% 2mm 33% 3mm	Case 4 100% 3mm-diameter air bubbles
Total number of scatters	N	0.87 N	0.67 N	0.30 N
$N\sigma_b$ term in eq.(4.19)	$N\sigma_b$	1.69 $N\sigma_b$	2.76 $N\sigma_b$	3.38 $N\sigma_b$
K_3	K_e	1.46 K_e	2.17 K_3	2.58 K_e
$1-1/L^2$	$1-1/L^2$	$1.16(1-1/L^2)$	$1.26(1-1/L^2)$	$1.29(1-1/L^2)$
$\sigma^\circ_v(\theta')$	$\sigma^\circ_v(\theta')$	σ°v + 1.3 dB	σ°v + 2.1 dB	σ°v + 2.3 dB

cross section of individual elements increases as(radius)^6. However, for a given density of ice, the number of scatterers has to decrease as(radius)^3. Therefore the term N $\angle_b$ in Eq.(4) increases as (radius)^3. As the scattering cross section increases, the extinction coefficient increases as well. The relative increase in k_e depends on the scattering albedo. Also as k_e increases the loss L increases, thereby increasing the term$(1- 1/L^2)$ in Eq.(4). When there are scatterers with various sizes, the problem gets more complicated. Table 1 summarizes the results for several cases of air-bubble size distribution. The parameters used are: ϵ_b = 3.15-j 0.01, density = 0.7 gm/cm^3, depth=

20 cm, and frequency = 13 GHz. If 10% of the air bubbles are larger(3 mm in diameter) than the 2 mm air bubbles, the σ° can be up to 1.3 dB higher.

The density of multiyear ice usually increases with depth. This can either be modeled as; (1)the number of air bubbles decreases with depth, or (2)the size of air bubbles decreases with depth. In this paper, only the first case is considered. When the density profile is given as a function of depth, $\rho = \rho(z)$, the corresponding number of scatterers per unit volume changes with depth, and so does the extinction coefficient. This problem can be evaluated numerically if $\rho(z)$ is given. Alternatively, the following simple approximation seems to be better when one considers the difficulties associated with measurements of the density of sea ice.

Let us assume that the measured density profiles show a linear increase with depth from 0.7 to 0.8 gm/cm^3. The average density is 0.75 gm/cm^3, and this layer can be divided into two layers of equal depth with densities of 0.7 and 0.8 gm/cm^3 respectively, maintaining the same average density. Let σ_1° be the volume scattering coefficient of the first-layer, and σ_2° be that of the second layer. Then the total volume scattering coefficient σ_v° is,

$$\sigma_v^\circ = \sigma_1^\circ + \sigma_2^\circ / L_1^2$$
$$= \frac{N_1 \sigma_b \cos\theta'}{2 k_{e1}} \left(1 - \frac{1}{L_1^2}\right) + \frac{N_2 \sigma_b \cos\theta'}{2 k_{e2}} \left(1 - \frac{1}{L_2^2}\right) \frac{1}{L_1^2} \quad \ldots\ldots\ldots\ldots\ldots\ldots (5)$$

where L_i is the one-way loss through the i-th layer. This concept can be extended further to divide the layer into smaller sublayers, and

$$\sigma_v^\circ = \sigma_1^\circ + \sigma_2^\circ / L_1^2 + \sigma_3^\circ / (L_1 L_2)^2 + \sigma_4^\circ / (L_1 L_2 L_3)^2 + \ldots\ldots\ldots\ldots\ldots\ldots (6)$$

Table 2 summarizes the results for several approximations which all have the same average densities and same size scatterers. As can be seen from the table, the approximation of assuming the constant density for the whole layer gives satisfactory results when compared to the results of decomposing the layer into multiple layers with varying densities.

The concept of adding the contribution of several layers to get the effective volume scattering coefficient can be used to see the effect of small air bubbles which are found throughout the multiyear ice below the main scattering layer. The clear ice region has higher density(0.85–0.9 gm/cm^3) and smaller air bubbles(diameter of less than 1 mm) than the first layer. Moreover, the loss increases due to non-zero salinity. At 13 GHz, the contribution of the secondary layer of 50 cm thick with $\rho = 0.85$ gm/cm^3, and the air bubbles of diameter = 1 mm is about 17 dB lower than that of the main 20 cm-deep scattering layer with $\rho = 0.75$ gm/cm^3, and air bubbles of

Table 2. Effect of Density Variations

	One Layer 20 cm	Two Layers 10 cm each	Three Layers 6.7 cm each	Four Layers 5 cm each
	$\rho = 0.75$ gm/cm^3 scatterer dia. = 2 mm	$\rho_1 = 0.7$ $\rho_2 = 0.8$	$\rho_1 = 0.7$ $\rho_2 = 0.75$ $\rho_3 = 0.8$	$\rho_1 = 0.7$ $\rho_2 = 0.733$ $\rho_3 = 0.766$ $\rho_4 = 0.8$
Number of scatterers per unit vol.	N	$N_1 = 1.28$ N $N_2 = 0.72$ N	$N_1 = 1.28$ N $N_2 = N$ $N_3 = 0.72$ N	$N_1 = 1.28$ N $N_2 = 1.1$ N $N_3 = 0.9$ N $N_4 = 0.72$ N
$\sigma^\circ_v(\theta')$	$\sigma^\circ_v(\theta')$	$\sigma^\circ_v + 0.19$(dB)	$\sigma^\circ_v + 0.17$(dB)	$\sigma^\circ_v + 0.16$(dB)

diameter = 2 mm(Kim, 1984). The effect of the secondary layer with small air bubbles seems negligible; therefore, the multiyear ice can be modeled as a single layer of air bubbles.

So far, the volume-scattering contribution from multiyear ice has been considered. The term $T^2\ \sigma^\circ_v$ in eq.(3) has been shown to be able to approximate the complicated theoretical volume-scattering formulation(intensity approach). However, the measured σ° always includes the purely surface-scattered term, and as shown in the previous section, it may be an important part of the total backscattering especially at small incidence angles and at lower frequencies than about X-band. The σ°_s term in eq.(3) is calculated using the physical-optics model(Kim, 1984), and added to the semi-empirical volume scattering term, $T^2\ \sigma^\circ_v$, to get the backscattering coefficient for multiyear ice.

Fig. 9 shows the calculated frequency behavior of σ° for multiyear ice at several incidence angles. Also shown are the measured multiyear ice data. Unfortunately, no supporting ice characteristics are available, and the model parameters were selected arbitrarily within typical reported values to match the data at the incidence angle of 40°. More scatter in the data at low frequencies(C-band) as can be seen in Fig.9 might be due to the variations in the surface roughness, since at low microwave frequencies the surface-scattering may be the dominant backscattering mechanism for multiyear ice even at angles away from vertical(see Fig. 5).

Fig. 10 shows the calculated and measured angular response at several frequencies. The model parameters are same as those shown in Fig. 9(frequency response). At 13.6 GHz, the main contribution is from the volume(characterized by a very slow angular drop-off), while at 5.2 GHz, the surface-scattering is dominant. Even though the model parameters are not optimized in any sense, a good general agreement can be seen in both the frequency – and angular-behaviors.

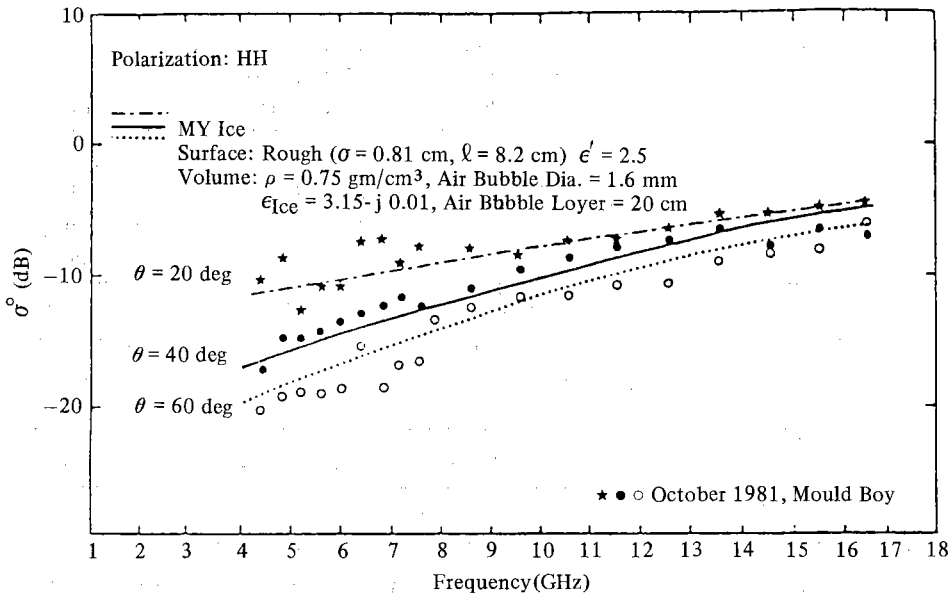

Fig. 9. Measured and Predicted σ° of Multiyear Ice. The model parameters are chosen to match the data at 40°.

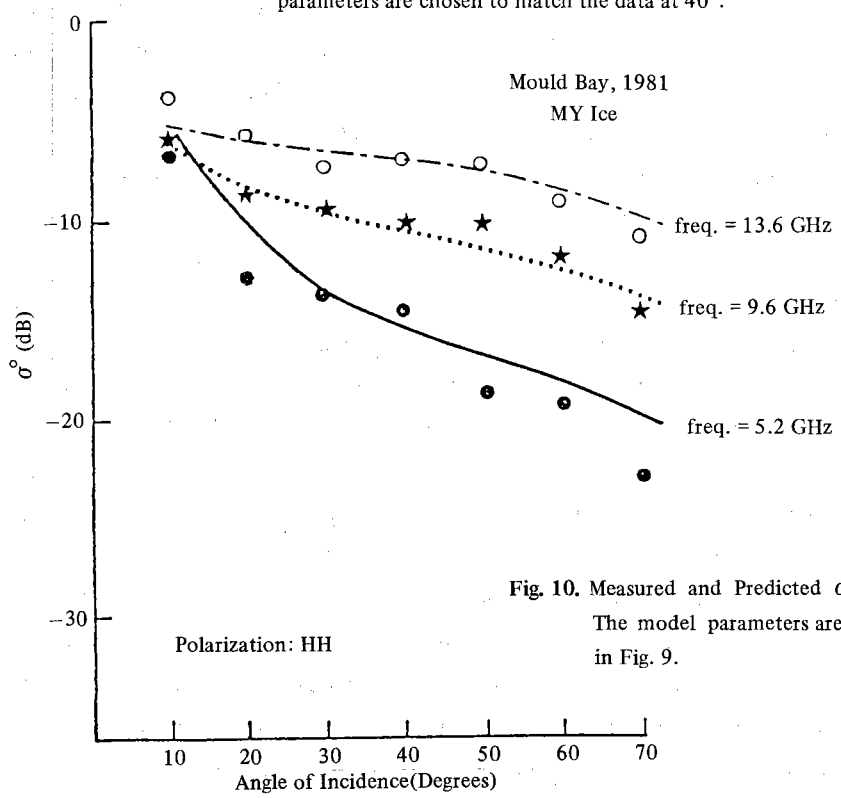

Fig. 10. Measured and Predicted σ° of Multiyear Ice. The model parameters are same as those shown in Fig. 9.

4. Conclusions

In this paper and the companion paper, angular–, frequency–, and polarization-dependence of σ° for two major types of sea ice(first-year and multiyear ice) in cold conditions were investigated. The assumption was tested that the surface scattering is the dominant backscattering mechanism for first-year ice, and that the volume scattering is dominant for multiyear ice.

A scattering volume can be modelled either as a continuous random medium characterized with correlation lengths and variances, or as a discrete medium embedded with random scatterers characterized with scattering albedo and optical depth. In this study the latter approach was adapted using the radiative-transfer model, and the air bubbles in the recrystallized ice layer in the top portion of the multiyear ice were assumed to be the primary volume scatterers. The surface scattering is always present, and when the frequency is below about X-band, it was shown that the volume-scattering contribution can be smaller than the surface-scattering contribution. The backscattered power is the sum of these two; this sum provides a good general agreement to the measured frequency- and angular-behaviors of σ° of multiyear ice, although the model neglected the effect of ridging, meltponds, and snow cover.

The complicated theoretical solution of the radiative-transfer equation reduces to a simple analytical solution if the multiple scattering and the volume-surface interaction can be neglected. The volume backscattering coefficient given by the sum of the backscattering coefficients of all the single scatterers was shown to be a good approximation to the value calculated with the radiative-transfer equation. Using the simple model, the effect of the nonuniformity of the size of the air bubbles, and also the variation of ice density with depth were studied. It was shown that the minor variation in the size of the air bubbles has insignificant effect on volume backscattering coefficient. Also it was shown that the approximation of assuming the constant density for the whole scattering layer gives satisfactory result when compared to the results of decomposing the layer into multiple layers with varying densities.

In Kim et al.(1985), the models described in this paper were used to identify the optimum radar paramters for sea ice monitoring. The possible ranges of σ° under various conditions(surface roughness, salinity, temperature, density, and air bubble size) were calculated for multiyear and first-year ice by adjusting the parameters within reported ranges of values. Although the calculations showed no specific resonance that would favor any particular frequency or incidence angle, the result confirmed the experimental findings that Ku- and X-band frequencies are better than lower frequencies, and that the incidence angles larger than about 30 to 40 degrees are better for discriminating multiyear ice from first-year ice, at least when melting is not occuring.

References

1) Cambell W. J., R. O. Ramseier, P. Gloersen, M. L. Bryan, et al., 1978. Microwave Remote Sensing of Sea Ice in the AIDJEX Main Experment. *Boundary Layer Meteorology,* **13,** pp.309-337.

2) Eom, H. J., 1982. *Theoretical Scatter and Emission Models for Microwave Remote Sensing,* Ph. D. Thesis, University of Kansas, Lawrence, Kansas.

3) Gray, A. L., R. O. Ramseier and W. J. Campbell, 1977. *Scatterometer and SLAR Results Obtained over Arctic Sea Ice, Presented to the 4th Canadian Symposium on Remote Sensing,* Quebec City, Canada.

4) Gray, A. L., R. K. Hawkins, C. E. Livingstone, L. D. Arsenault and W. M. Johnstone, 1982. Simultaneous Scatterometer and Radiometer Measurements of Sea Ice Microwave Singnatures, *IEEE J. Ocean Engrg.,* Vol. OE-7(1), pp.20-30.

5) Karam, M. A. and A. K. Fung, 1982. Propagation and Scattering in Multi-Layered Radom Media with Rough Interfaces. *Electromagnetics* 2. pp.239-256.

6) Kim, Y. S., 1984. *Theoretical and Experimental Study of Radar Backscatter from Sea Ice,* Ph. D. Thesis, University of Kansas, Lawrence, Kansas.

7) Kim, Y. S., R. G. Onstott and R. K. Moore, 1984. The Effect of Snow Cover on Microwave Backscatter from Sea Ice. *IEEE J. of Ocean Eng.,* Vol. OE-9, pp.383-388.

8) Kim, Y. S., R. Moore, R. Onstott and S. Gogineni, 1985. Toward the Identification of Optimum Radar Parameters for Sea Ice Monitoring, *J. Glacio.,* Vol. 31(109), pp.214-219.

9) Onstott, R. G., 1980. *Radar Backscatter Study of Sea Ice,* Ph. D. Thesis, University of Kansas, Lawrence, Kansas.

10) Poe, G. A., Stogryn, A. T. Edgerton and R. O. Ramseier, 1974. Aerojet Electrosystems Co. *Final Report,* No. 1804 FR-1.(Unpublished).

11) Troy, B. E., J. P. Hollinger, R. M. Lerner, and M. M. Wisler, 1981. Measurement of the Microwave Properties of Sea Ice at 90GHz and Lower Frequencies. *J. Geo. Res.,* Vol. 86, No. C5, pp.4283-4289.

12) Vant, M. R., R. G. Gray, R. O. Ramseier and V. Makios, 1974 Dielectric Properties of Fresh and Sea Ice at 10 and 35 GHz. *J. Appl. Phys.,* Vol. 45, No. 11, pp.4712-4717.

13) Vant, M. R., R. O. Ramseier and V. Makios, 1978. The Complex Dielectric Constant of Sea Ice at Frequencies in the Range 0.1-40 GHz. *J. Appl. Phys.,* Vol. 49(3), pp.1264-1280.